Alkenyl-functionalized NHC iridium-based catalysts for hydrosilylation†

Alessandro Zanardi, Eduardo Peris and Jose A. Mata*

A family of alkenyl-functionalized *N*-heterocyclic-carbene–iridium(I) complexes has been synthesized, providing a series of mono-coordinated, bis-chelate and *pincer* alkenyl-NHC species. Olefin coordination is highly influenced by the nature of the substituents on the NHC ring, and on the length of the alkenyl branch. A fluxional process involving coordination/decoordination of the olefin in bis-allyl-NHC complexes has been studied, and the activation parameters have been determined by means of VT-NMR spectroscopy. The mono-coordinated complexes are highly active in the hydrosilylation of terminal alkynes, showing high selectivity for the *Z*-isomers, with no α-isomers or dehydrogenative silylation processes being observed. The molecular structures reported that are representative of the species have been determined by means of X-ray crystallography.

Introduction

The hydrosilylation of unsaturated organic molecules is one of the most powerful tools for the transformation of organic compounds, providing a wide range of industrial applications.[1] Organosilicon compounds are important functional groups because their derivation into other functionalities through the oxidative cleavage of the carbon–silicon bond is easily achieved.[2] The versatility of catalytic hydrosilylation towards the reduction of carbon–carbon, carbon–oxygen and carbon–nitrogen multiple bonds is a 100% atom-economical and efficient process. The search for catalysts that can promote hydrosilylation processes under mild and aerobic conditions is one of the main aims of industry.[3] An important drawback of the hydrosilylation process in the laboratory is that there remain no clear patterns in the design of highly selective catalysts, so the search for new complexes providing selective processes is highly desirable.

N-Heterocyclic carbene (NHC) ligands are finding increasing use in organometallic chemistry and homogeneous catalysis.[4] Part of this success is due to the electron donor ability of NHC ligands, which is higher than that of phosphines.[5] We have been interested in the use of polydentate NHCs and their application in catalysis,[6] as well as the influence of their anisotropic nature in the reactivity patterns of their complexes.[7] As part of our research, we focused our attention on the preparation of M–NHC complexes as hydrosilylation catalysts,[8] and also studied the mechanism of the process by means of electrospray mass spectroscopy.[9] Based on our previous results, we now report the syntheses of a series of NHC–Ir(I) complexes functionalized with terminal alkenes.

The original idea of our work came from the interesting recent reports of Hahn *et al.*, who described a series of Ir complexes with allyl- and bis-allyl-NHC ligands, some of them tested in transfer hydrogenation to cyclohexanone (Scheme 1).[10,11] We thought that changing the nature of the NHC ligand by substituting the 4 and 5 positions of the azole ring, and modifying the length of the terminal alkenyl groups may provide an interesting opportunity to systematically study the reactivity pattern of the system. In our study, we observed that some of the complexes obtained showed a fluxional behaviour, which we studied by means of variable temperature NMR (VT-NMR) experiments. More remarkably, the NHC–Ir(I) complexes are highly active and selective catalysts in the hydrosilylation of terminal alkynes.

Results and discussion

Syntheses and characterization

Transmetallation of the corresponding silver–NHC compounds to [IrCl(COD)]₂ afforded complexes **1a**, **1b** and **1c** (60–90%). A compound similar to **1a**, but with a bromine ligand instead of a chlorine, had been previously obtained by the direct reaction of 1,3-bis(2-propenyl)imidazolium bromide with [Ir(μ-OMe)(COD)]₂.[11] The addition of AgBF₄ to corresponding solutions of **1** in acetone provided the corresponding carbene-bisolefin pincer species **2**. All compounds obtained were characterized by the usual spectroscopic techniques, elemental analysis and/or high resolution mass spectroscopy.
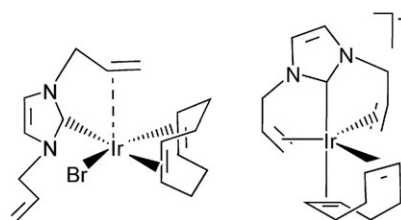
Departament Química Inorgànica i Orgànica, Universitat Jaume I, Av. Vicent Sos Baynat s/n, E-12071 Castelló, Spain. E-mail: jmata@qio.uji.es; Fax: +34 964728214; Tel: +34 964728234
† Electronic supplementary information (ESI) available: Description of general procedures, ligand precursor syntheses, catalytic studies, NMR characterization (¹H, ¹³C, COSY), VT-NMR experiments and experimental crystallographic data collection. See DOI: 10.1039/b707280e
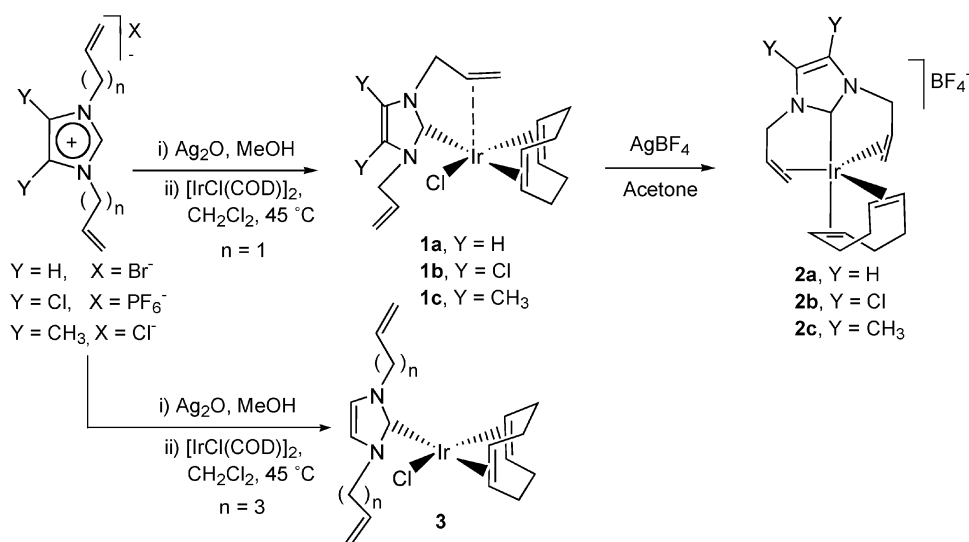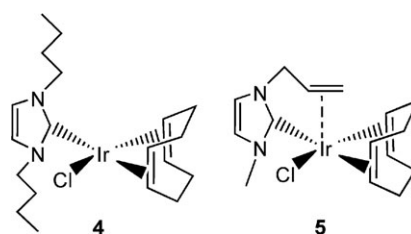

Scheme 1

Scheme 2

Complexes **1a**, **1b** and **1c** show interesting examples of fluxional behavior. In the case of **1a**, we were able to obtain the activation barrier parameters by means of VT-NMR studies. The room temperature ^{1}H NMR spectrum of complex **1a** shows a different environment for the two azole ring protons at 6.89 and 6.67 ppm. This observation and the low frequency alkene resonances are consistent with the coordination of one of the olefinic fragments. The upper and lower sides of the iridium complex are different, making all the residences magnetically inequivalent. The signals due to the olefinic protons at room temperature are broad (*e.g.* 6.89 ppm, $w_{\frac{1}{2}}$ = 9.43 Hz; solvent CDCl$_3$, $w_{\frac{1}{2}}$ = 0.98 Hz), suggesting that a fluxional process is operating that involves the chemical exchange of the coordinated and uncoordinated olefins. Metal–carbene rotation is not feasible, as previously observed in analogous rhodium complexes.[12,13] Previous studies by Enders and co-workers showed that hindered rotation is found for NHC–rhodium(I) complexes with bulky cyclooctadiene or norbornadiene ligands.[14] A combination of linewidth analysis and the coalescence temperature of the signals corresponding to the protons of the imidazolylidene ring (see the ESI†) allowed us to establish the kinetic parameters as $\Delta H^{\neq}$ = 20.9 Kcal mol^{-1} and $\Delta S^{\neq}$ = 17.4 cal mol^{-1} K^{-1}. The decoordination of the olefin being the main factor governing the process, we estimate that the $\Delta H^{\neq}$ value of 20.9 kcal mol^{-1} is a good estimation of the Ir–olefin bond energy. This analysis is in good agreement with experimental and theoretical data for olefin-coordinated complexes.[15] The high positive value of $\Delta S^{\neq}$ may suggest a highly disordered transition state compared to the ground state, probably as a consequence of the decoordination of the olefinic branch. A variable temperature study of complex **1a** was carried out by ^{13}C NMR spectroscopy, confirming the above mentioned kinetic parameters.

In order to check whether longer alkenyl branches would provide chelating Ir(I) species, we decided to obtain the related complex, using 1,3-bis(4-pentenyl)imidazolium bromide as the carbene precursor. The coordination of this imidazolium salt to [IrCl(COD)]$_2$ was achieved by the same methodology as the one shown in Scheme 2, but in this case only the monodentate

species was obtained, with both alkenyl branches being out of the coordination sphere of the metal. The addition of AgBF$_4$ to the complex did not afford the desired carbene–olefin chelating species, thus suggesting that olefin coordination must be an unfavorable process due to the formation of the more unstable seven membered ring. We recently observed a similar behaviour for other alkenyl-NHC species of Cp*Ir(III).[16] For comparative reasons, in the catalytic studies (see below), we found it convenient to obtain complexes **4**[13] and **5**[11] by following the procedures mentioned above (Scheme 3).

Scheme 3

X-Ray diffraction studies

Crystals of **2a**, **2b**·**PF$_6$** and **3** suitable for X-ray diffraction analysis were obtained by slow evaporation from corresponding concentrated dichloromethane–hexanes solutions. The structures of **2a** and **2b**·**PF$_6$** confirm the pincer coordination of the NHC ligand, a result of the binding of the two olefins.‡ The geometry at the iridium center (Fig. 1 and Fig. 2) is best described as distorted trigonal bipyramidal. The equatorial plane is defined by the two olefinic fragments from the NHC-bis-allyl ligand and one C=C from COD, while the axial axis is occupied by the other C=C from COD and the carbene carbon. The relative orientation of the olefin fragments of the
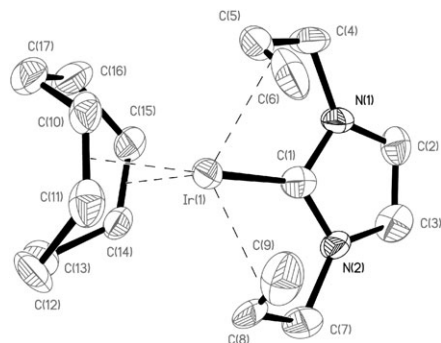
Fig. 1 The ORTEP diagram of complex **2a**, showing 50% probability ellipsoids. Hydrogen atoms and the counterion (BF_4^-) have been omitted for clarity. Selected bond lengths (Å) and angles (°): Ir(1)–C(1) = 1.934(9), Ir(1)–C(5) = 2.214(8), Ir(1)–C(9) = 2.261(9), Ir(1)–C(8) = 2.308(8), Ir(1)–C(6) = 2.225(9), C(5)–C(6) = 1.404(12), C(8)–C(9) = 1.373(13); N(1)–C(1)–Ir(1) = 123.9(7), N(1)–C(4)–C(5)–C(6) = 57.7(11).

bis-allyl ligand is *syn*, with the two olefins being symmetry-related by a plane perpendicular to the azole ring.

The structure of compound **3** confirms that the olefin fragment of the NHC remains unbound (Fig. 3).‡ The geometry at the iridium center is pseudo-square planar. The plane angle defined by the azole ring is almost perpendicular to the iridium coordination plane ($\alpha = 84.2°$ for **3**).

The pincer coordination of the NHC-bis-allyl ligand seems to push the azole ring closer to the metal center, shortening the Ir–$C_{carbene}$ distance by *ca.* 0.1 Å. As a consequence, the iridium–carbene distance is in the expected range for complex **3** (Ir–$C_{carbene}$ = 2.030(10) Å), but slightly shorter for complexes **2a** (1.934(9) Å) and **2b·PF$_6$** (1.944(12) Å). All metal-coordinated olefins show a longer C=C distance compared to the free alkene ($d_{C=C}$, 1.337 Å) as a consequence of metal back-bonding into the olefin π* orbital.

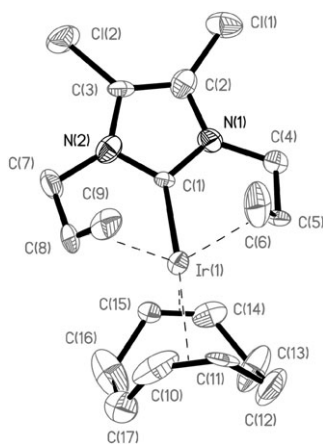**Fig. 2** The ORTEP diagram of complex **2b·PF$_6$**, showing 50% probability ellipsoids. Hydrogen atoms and the counterion (PF_6^-) have been omitted for clarity. Selected bond lengths (Å) and angles (°): Ir(1)–C(1) = 1.944(12), Ir(1)–C(5) = 2.221(14), Ir(1)–C(6) = 2.248(18), Ir(1)–C(8) = 2.247(12), Ir(1)–C(9) = 2.203(12), C(5)–C(6) = 1.38(2), C(8)–C(9) = 1.41(2); N(1)–C(1)–Ir(1) = 124.5(9), N(1)–C(4)–C(5)–C(6) = −56.8(17).
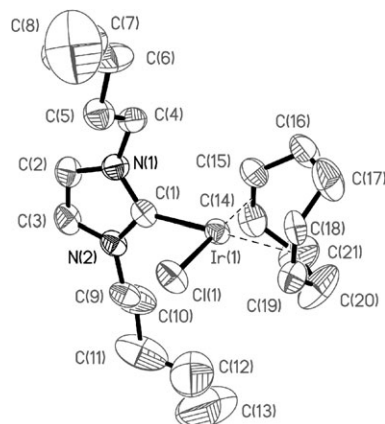

Fig. 3 The ORTEP diagram of complex **3**, showing 35% probability ellipsoids. Hydrogen atoms have been omitted for clarity. Selected bond lengths (Å) and angles (°): Ir(1)–C(1) = 2.030(10); N(1)–Ir(1)–C(1) = 127.6(7), N(1)–C(4)–C(5)–C(6) = −173.6(9); $\alpha = 84.2$ (α = angle between the imidazolium ring plane and the xy plane of the metal complex).

Catalytic hydrosilylation

Table 1 summarizes the catalytic results for the hydrosilylation of 1-hexyne with phenylacetylene using catalysts **1** and **3–5** at room temperature after 1 h of reaction. All the compounds showed some activity under the reaction conditions used (1 mol% cat. loading), the best conversions (68–92%) being obtained for catalysts **1a** and **5**. In general, the reaction proceeded with higher yields for the reduction of phenylacetylene, as has previously been reported,[17] although catalysts **3** and **4** seemed to present the reverse tendency. The 4,5-substituted azoles (**1b** and **1c**) presented a lower activity than their unsubstituted analogue (**1a**), although this behaviour did not seem to follow a logical tendency if we consider the electronic modification of the ligands implied.[18] In this sense, we believe that the 4,5-substituents may have had some steric influence on the reaction's outcome. The high selectivity of the products obtained is noteworthy, with a clear preference for the Z-isomer, which in some cases was obtained as the only product. This selectivity was higher when catalysts **1** (**1a**, **1b**

Table 1 Hydrosilylation of alkynes at room temperature (hydrosilane = HSiMe$_2$Ph)[a]

Entry	Catalyst[b]	Substrate	Conversion (%)[c]	α	E	Z
1	**1b**	1-Hexyne	21	—	—	100
2	**1a**	1-Hexyne	68	—	7	93
3	**1c**	1-Hexyne	25	—	—	100
4	**3**	1-Hexyne	71	—	12	88
5	**4**	1-Hexyne	46	—	9	91
6	**5**	1-Hexyne	55	—	17	83
7	**1b**	Phenylacetylene	57	—	34	66
8[d]	**1a**	Phenylacetylene	92	—	28	72
9	**1c**	Phenylacetylene	45	—	20	80
10	**3**	Phenylacetylene	18	—	7	93
11	**4**	Phenylacetylene	0			
12[d]	**5**	Phenylacetylene	80	—	20	80

[a] Temperature 25 °C, time 1 h, solvent CHCl$_3$. [b] Catalyst loading (1 mol%). [c] Yields determined by ^{1}H NMR. [d] Catalyst active for at least three runs.

Table 2 Hydrosilylation of phenylacetylene at 60 °C (hydrosilane = HSiMe$_2$Ph)^a

Entry	Catalyst^b	Time/h	Conversion (%)^c	α	E	Z
1	**1b**	1	70	—	10	90
2	**1a**	1	100	—	23	77
3	**1c**	1	67	—	12	88
4	**3**	1	36	—	21	79
5	**4**	1	55	—	26	74
6	**5**	1	100	—	27	73
7	**1b**	2	100	—	23	76
8	**1a**	2	100	—	17	83
9	**1c**	2	100	—	20	80
10	**3**	2	100	—	20	80
11	**4**	2	100	—	31	69
12	**5**	2	100	—	35	65
13	**1a**^{d}	2	85	—	30	70
14	**1a**^{e}	2	45^f	—	35	65

^{a} Temp 60 °C, Solvent CHCl$_3$. ^{b} Catalyst loading (1 mol%) unless otherwise stated. ^{c} Yields determined by ^{1}H NMR. ^{d} Catalyst loading (0.1 mol%). ^{e} Catalyst loading (0.01 mol%). ^{f} Full conversion was achieved after 24 h.

and **1c**) were used, compared to the selectivities shown by **5** (*i.e.*, compare entries 1–3 and 6 in Table 1). We believe that the second alkenyl branch of catalyst in **1** may have had some steric influence on the selectivity of the reaction. Compound **5**, with a small methyl group as a wingtip, had a reduced steric influence that seemed to reduce the selectivity of the process (although still high). In general, the selectivities obtained when using these catalysts were the highest we have obtained compared to similar Ir(I)– and Rh(I)–NHC species,[19] and lie among the highest reported to date for Ir complexes. Remarkably, the α-isomer was not obtained in any experiment. Degradation of the catalytically-active species was not observed in the hydrosilylation process, even at the end of the catalytic reaction. After the initial batch, two more runs using catalyst **1a** were carried out without any measurable deactivation of the system, confirming the high stability of the NHC–metal complexes (Table 1, entries 8 and 12).

Table 2 shows the results of the catalytic hydrosilylation of phenylacetylene at 60 °C. As expected, an increase of the reaction temperature resulted in an increase in reaction yields, with catalysts **1a** and **5** again achieving the highest efficiencies in terms of conversion (full in all cases). The selectivity for the Z-hydrosilylated isomer was reduced, but the reaction remained highly selective. Conversions between 65–90% lead to this reaction product, and only the β-isomers were obtained. Catalyst loadings as low as 0.1 and 0.01 mol% also provided high activities at 60 °C, although slow kinetics were found (Table 2, entries 13 and 14).

According to the results of this catalytic survey, olefin-functionalized NHC–iridium complexes constitute a new family of catalysts for the addition of Si–H to alkynes. The high activity and selectivity indicate the potential of these catalysts for future applications. VT-NMR studies revealed that the olefin coordination/decoordination fluxional process is enthalpy driven. The thermodynamic parameters are in agreement with the experimental and theoretical data for olefin coordination. Compound **1a** is a highly active and robust catalyst for the hydrosilylation of alkynes because it combines the high activity of iridium with the stability of the

NHC ligand. Further studies related to the electronic and steric effects of olefin-functionalized NHC spectator ligands are in progress.

Experimental section

General procedure

Ligand precursors were prepared according to literature methodologies.[20] Experimental conditions and characterization data can be found in the ESI.† NMR Spectra were recorded on Varian Inova 300 and 500 MHz instruments using CDCl$_3$ as the solvent. Elemental analyses were carried out in a Euro EA 3000 Eurovector Analyser. Electrospray Mass Spectra (ESI-MS) were recorded on a Micromass Quatro LC instrument, nitrogen being employed as the drying and nebulising gas. All other reagents were used as received from commercial suppliers.

1,3-Bis(2-propenyl)-imidazolin-2-ylidene [(1,2,5,6-η)-1-5-cyclooctadiene]chloro iridium (1a). Silver oxide (63 mg, 0.27 mmol) was added to a solution of 1,3-bis(2-propenyl)imidazolium bromide (55 mg, 0.3 mmol) in MeOH. The solution was stirred at room temperature for 1 h and filtered through Celite®. The solution was concentrated under reduced pressure and redissolved in dichloromethane. [IrCl(COD)]$_2$ (100 mg, 0.15 mmol) was added and the mixture was stirred for 1 h at 45 °C. After solvent removal, the crude product was purified by flash chromatography using CH$_2$Cl$_2$/MeOH (7 : 3) as the eluent (yield 117 mg, 80%).

^{1}H NMR (500 MHz, CDCl$_3$, $T = -15$ °C): δ 6.89 (s, 1H, NCHCHN), 6.67 (s, 1H, NCHCHN), 5.92 (m, 1H, NCH$_2$CH=CH$_2$, not coordinated), 5.52 (dd, $^3J_{HH}$ = 4.5 Hz, $^2J_{HH}$ = 17.0 Hz, 1H, NCHHCH=CH$_2$, not coordinated), 5.13 (d, $^3J_{HH}$ = 10.5 Hz, 1H, NCH$_2$CH=CHH$_{cis}$, not coordinated), 4.89 (d, $^3J_{HH}$ = 17 Hz, NCH$_2$CH=CHH$_{trans}$, not coordinated), 4.66 (m, 2H, NCHHCH=CH$_2$, not coordinated and COD), 4.23 (m, 2H, NCHHCH=CH$_2$, coordinated and NCH$_2$CH=CH$_2$, coordinated), 3.70 (d, $^3J_{HH}$ = 15 Hz, NCHHCH=CH$_2$, coordinated), 3.54 (m, 1H, COD), 3.44 (m, 1H, COD), 2.93 (m, 1H, COD), 2.70 (m, 2H, COD), 2.49 (m, 1H, COD), 2.39 (m, 2H, COD), 2.08 (d, 1H, $^3J_{HH_{cis}}$ = 7.5 Hz, NCH$_2$CH=CHH, coordinated), 1.93 (m, 2H, COD), 1.89 (d, 1H, $^3J_{HH_{trans}}$ = 9.0 Hz, NCH$_2$CH=CHH), 1.61 (m, 1H, COD). ^{13}C NMR (75 MHz, CDCl$_3$): δ 161.9 (NCN), 135.4 (NCH$_2$CH=CH$_2$, not coordinated), 122.2 (NCHCHN), 118.0 (NCHCHN), 117.5 (NCH$_2$CH=CH$_2$, not coordinated), 99.0, 97.7, 60.6, 55.6 (COD), 52.89 (NCH$_2$CH=CH$_2$, coordinated), 52.5 (NCH$_2$CH=CH$_2$, not coordinated), 47.27 (NCH$_2$CH=CH$_2$, coordinated), 41.0 (COD), 35.9 (NCH$_2$CH=CH$_2$, coordinated), 33.4, 29.6, 28.1 (COD). ESI-MS (cone 25 V): m/z (fragment): 449.4 [M − Cl$^+$].

4,5-Dichloro-1,3-bis(2-propenyl)imidazolin-2-ylidene [(1,2,5,6-η)-1-5-cyclooctadiene]chloro iridium (1b). The synthesis of complex **1b** was carried out using the same general procedure as described for complex **1a** using silver oxide (76 mg, 0.33 mmol), 4,5-dichloro-1,3-bis(2-propenyl)imidazolium hexafluorophosphate (89 mg, 0.30 mmol) and [IrCl(COD)]$_2$ (100 mg, 0.15 mmol) (yield 114 mg, 70%).

^{1}H NMR (500 MHz, CDCl$_3$): δ 5.97 (d, 1H, $^2J_{HH}$ = 17 Hz, NCH*H*CH=CH$_2$, not coordinated), 5.78 (m, 1H, NCH$_2$C*H*=CH$_2$, not coordinated), 5.08 (m, 1H, NCH$_2$CH=C*H*$_2$, not coordinated), 4.68 (m, 2H, NCH$_2$CH=C*H*$_2$, not coordinated), 4.46 (m, 1H, NCH*H*CH=CH$_2$, not coordinated), 4.13 (m, 2H, NCH*H*CH=CH$_2$, coordinated and NCH$_2$C*H*CH$_2$, coordinated), 3.77 (d, $^2J_{HH}$ = 11 Hz, NCH*H*CH=CH$_2$, coordinated), 3.59 (m, 1H, COD), 3.46 (m, 1H, COD), 3.34 (m, 1H, COD), 2.87 (m, 2H, COD), 2.68 (m, 1H, COD), 2.38 (m, 2H, COD), 2.28 (m, 1H, NCH$_2$CH=CH*H*, coordinated), 2.00 (m, 2H, COD), 1.91 (m, 1H, NCH$_2$CH=CH*H*), 1.58 (m, 2H, COD).

^{13}C NMR (75 MHz, CDCl$_3$): δ 161.61 (N*C*N), 134.05 (NCH$_2$*C*H=CH$_2$, not coordinated), Cl–C not observed, 115.87 (NCH$_2$CH=*C*H$_2$, not coordinated), 99.41, 97.96, 61.20, 56.06 (COD–CH), 52.36 (NCH$_2$CH=*C*H$_2$, coordinated), 50.55 (N*C*H$_2$CH=CH$_2$, not coordinated), 44.55 (N*C*H$_2$CH=CH$_2$, coordinated), 40.96 (COD–CH$_2$), 35.54 (N*C*H$_2$CH=CH$_2$, coordinated), 33.15, 28.80, 27.48 (COD). ESI-MS (cone 25 V): m/z (fragment) 517.1 [M − Cl]$^+$.

4,5-Dimethyl-1,3-bis(2-propenyl)imidazolin-2-ylidene [(1,2,5,6-η)-1-5-cyclooctadiene]chloro iridium (1c). The synthesis of complex **1c** was carried out using the same general procedure as described for complex **1a** using silver oxide (94 mg, 0.45 mmol), 4,5-dimethyl-1,3-bis(2-propenyl)imidazolium chloride (95 mg, 0.45 mmol) and [IrCl(COD)]$_2$ (150 mg, 0.22 mmol) (yield 148 mg, 66%).

^{1}H NMR (500 MHz, CDCl$_3$): δ 5.85 (m, 2H, NCH*H*CH=CH$_2$, NCH$_2$C*H*=CH$_2$, not coordinated), 5.03 (d, $^2J_{HH}$ = 15.5 Hz, 1H, NCH$_2$CH=C*H*$_2$, not coordinated), 4.60 (m, 1H, NCH$_2$CH=C*H*$_2$, not coordinated), 4.18 (m, 2H, COD, NCH*H*CH=CH$_2$, not coordinated), 4.01 (m, 2H, NCH*H*CH=CH$_2$, coordinated and COD), 3.61–3.43 (m, 4H, NCH*H*CH=CH$_2$, NCH$_2$C*H*=CH$_2$, coordinated and COD), 3.30 (m, 1H, COD), 2.95 (m, 2H, COD), 2.85 (m, 2H, COD), 2.38 (m, 1H, COD), 2.28 (m, 1H, NCH$_2$CH=CH*H*, coordinated), 2.06 (s, 3H, CH$_3$), 1.91 (m, 1H, NCH$_2$CH=CH*H*, coordinated), 1.89 (s, 3H, CH$_3$), 1.54 (m, 2H, COD). ^{13}C NMR (75 MHz, CDCl$_3$): δ 158.9 (N*C*N), 136.1 (NCH$_2$*C*H=CH$_2$, not coordinated), 125.8 (*C*–CH$_3$), 122.2 (*C*–CH$_3$), 114.5 (NCH$_2$CH=*C*H$_2$, not coordinated), 98.3, 96.7, 60.1, 55.3 (COD), 50.3 (NCH$_2$CH=*C*H$_2$, coordinated), 49.4 (N*C*H$_2$CH=CH$_2$, not coordinated), 46.1 (N*C*H$_2$CH=CH$_2$, coordinated), 41.2 (COD), 35.8 (N*C*H$_2$CH=CH$_2$, coordinated), 33.3, 29.0, 27.5 (COD), 9.7 (*C*H$_3$), 8.9 (*C*H$_3$). ESI-MS (cone 25 V): m/z (fragment) 477.2 [M − Cl]$^+$.

1,3-Bis(2-propenyl)-imidazolin-2-ylidene [(1,2,5,6-η)-1-5-cyclooctadiene]iridium tetrafluoroborate (2a). To a solution of complex **1a** (44 mg, 0.09 mmol) in acetone was added AgBF$_4$ (18 mg, 0.09 mmol), and the mixture was stirred at room temperature for 4 h. The suspension was filtered through Celite® and the solution concentrated under reduced pressure. Precipitation with diethyl ether (6 mL) afforded a solid (yield 40 mg, 82%).

^{1}H NMR (500 MHz, CDCl$_3$): δ 6.88 (s, 2H, NC*H*C*H*N), 5.19 (m, 2H, NCH$_2$C*H*=CH$_2$), 4.73 (m, 2H, COD), 4.60 (dd,

$^3J_{HH}$ = 5.0 Hz, $^2J_{HH}$ = 13.0 Hz, 2H, NCH*H*CH=CH$_2$), 4.40 (d, 2H, $^2J_{HH}$ = 13.5 Hz, NCH*H*CH=CH$_2$), 3.52 (m, 2H, COD), 3.47 (d, $^3J_{HH}$ = 9.0 Hz, 2H, NCH$_2$CH=CH*H*$_{cis}$), 2.85 (m, 2H, COD), 2.75 (d, $^3J_{HH}$ = 11.5 Hz, 2H, NCH$_2$CH=CH*H*$_{trans}$), 2.72 (m, 2H, COD), 2.29 (m, 4H, COD). ^{13}C NMR (75 MHz, CDCl$_3$): δ N*C*N not observed, 120.6 (N*C*H*C*HN), 93.7, 74.0 (COD), 64.9 (NCH$_2$*C*H=CH$_2$), 51.6 (N*C*H$_2$CH=CH$_2$), 42.6 (NCH$_2$CH=*C*H$_2$), 32.8, 31.4 (COD). ESI-MS (cone 25 V): m/z (fragment) 449.1 [M]$^+$.

4,5-Dichloro-1,3-bis(2-propenyl)imidazolin-2-ylidene [(1,2,5,6-η)-1-5-cyclooctadiene]iridium hexafluorophosphate (2b · PF$_6$). The synthesis of complex **2b** was carried out using the same general procedure as described for complex **2a** but followed by anion exchange (PF$_6$$^-$) using complex **1b** (75 mg, 0.13 mmol) and AgBF$_4$ (25 mg, 0.13 mmol) (yield 68 mg, 92%).

^{1}H NMR (500 MHz, CDCl$_3$): δ 5.22 (m, 2H, NCH$_2$C*H*=CH$_2$), 4.91 (m, 2H, COD), 4.55 (dd, $^3J_{HH}$ = 4.5 Hz, $^2J_{HH}$ = 13.5 Hz, 2H, NCH*H*CH=CH$_2$), 4.35 (d, $^2J_{HH}$ = 13.0 Hz, 2H, NCH*H*CH=CH$_2$), 3.59 (m, 2H, COD), 3.51 (d, $^3J_{HH}$ = 6.5 Hz, 2H, NCH$_2$CH=CH*H*$_{cis}$), 2.88 (d, $^3J_{HH}$ = 10 Hz, 2H, NCH$_2$CH=CH*H*$_{trans}$), 2.86 (m, 2H, COD), 2.73 (m, 2H, COD), 2.26 (m, 4H, COD). ^{13}C NMR (125 MHz, acetone): δ 161.25 (N*C*N), 114.6 (Cl–C), 94.82, 74.53 (COD), 63.71 (NCH$_2$*C*H=CH$_2$), 51.11 (N*C*H$_2$CH=CH$_2$), 42.60 (NCH$_2$CH=*C*H$_2$), 32.26, 30.87 (COD). ESI-MS (cone 25 V): m/z (fragment) 517.0 [M]$^+$.

4,5-Dimethyl-1,3-bis(2-propenyl)imidazolin-2-ylidene [(1,2,5,6-η)-1-5-cyclooctadiene]iridium hexafluorophosphate (2cPF$_6$). The synthesis of complex **2c** was carried out using the same general procedure as described for complex **2a** but followed by anion exchange (PF$_6$$^-$ using complex **1c** (40 mg, 0.08 mmol) and AgBF$_4$ (15 mg, 0.08 mmol) (yield 30 mg, 68%).

^{1}H NMR (500 MHz, CDCl$_3$): δ 5.17 (m, 2H, NCH$_2$C*H*=CH$_2$), 4.74 (m, 2H, COD), 4.44 (dd, $^3J_{HH}$ = 4.5 Hz, $^2J_{HH}$ = 13.0 Hz, 2H, NCH*H*CH=CH$_2$), 4.21 (d, $^2J_{HH}$ = 12.5 Hz, 2H, NCH*H*CH=CH$_2$), 3.47 (m, 2H, COD), 3.44 (d, $^3J_{HH}$ = 8.0 Hz, 2H, NCH$_2$CH=CH*H*$_{cis}$), 2.85 (m, 2H, COD), 2.77 (d, $^3J_{HH}$ = 12.0 Hz, 2H, NCH$_2$CH=CH*H*$_{trans}$), 2.70 (m, 2H, COD), 2.29 (m, 4H, COD), 1.98 (s, 6H, CH$_3$). ^{13}C NMR (125 MHz, CDCl$_3$): δ N*C*N not observed, 124.7 (*C*–CH$_3$), 93.3, 74.2 (COD), 63.9 (NCH$_2$*C*H=CH$_2$), 49.2 (N*C*H$_2$CH=CH$_2$), 42.2 (NCH$_2$CH=*C*H$_2$), 32.7, 31.3 (COD), 9.4 (CH$_3$). ESI-MS (cone 25 V): m/z (fragment) 477.3 [M]$^+$.

1,3-Bis(4-pentenyl)-imidazolin-2-ylidene [(1,2,5,6-η)-1-5-cyclooctadiene]chloro iridium (3). Silver oxide (63 mg, 0.27 mmol) was added to a solution of 1,3-bis(4-pentenyl) imidazolium bromide (85 mg, 0.30 mmol) in MeOH. The mixture was stirred at room temperature for 1 h and filtered through Celite®. The solution was concentrated under reduced pressure and redissolved in dichloromethane. [IrCl(COD)]$_2$ (100 mg, 0.15 mmol) was added and the mixture was stirred for 1 h at 45 °C. The volatiles were removed under reduced pressure. Compound **3** was obtained as a yellow oil (yield 122 mg, 77%).

^{1}H NMR (500 MHz, CDCl$_3$): δ 6.83 (s, 2H, C*H* imidazole), 5.86 (m, 2H, –C*H*=CH$_2$), 5.14 (m, 4H, –CH=C*H*$_2$), 4.58 (s, 2H, COD), 4.36 (m, 2H, –NC*H*$_2$–), 4.30 (m, 2H, –NC*H*$_2$–), 2.88 (s, 2H, COD), 2.19 (m, 4H, COD), 2.0 (m, 4H, COD),

Table 3 Crystal data and structure refinement for complexes **2a**, **2b · PF$_6$** and **3**

	2a	**2b · PF$_6$**	**3**
Empirical formula	C$_{17}$H$_{24}$BF$_4$IrN$_2$	C$_{17}$H$_{22}$Cl$_2$F$_6$IrN$_2$P	C$_{21}$H$_{32}$ClIrN$_2$
Molecular weight	535.39	662.44	540.14
Temperature/K	293(2)	293(2)	293(2)
Radiation (λ/Å)		Mo-K$_\alpha$ monochromated (0.71069)	
Crystal system	Monoclinic	Monoclinic	Triclinic
Space group	$P2(1)/c$ (no 14)	$P2(1)/c$ (no 14)	P-1 (no 2)
a/Å	8.1277(4)	15.2900(11)	12.0233(11)
b/Å	36.568(2)	10.7009(8)	13.9740(14)
c/Å	12.0502(6)	12.7347(10)	14.7666(15)
α/°	90	90	64.168(2)
β/°	99.5350(10)	96.789(2)	85.560(3)
γ/°	90	90	89.213(2)
Volume/Å^3	3532.0(3)	2069.0(3)	2225.8(4)
Z	8	4	4
Calc. density/g cm^{-3}	2.014	2.127	1.612
Absorption coefficient/mm^{-1}	7.602	6.848	6.124
$F(000)$	2064	1272	1064
Crystal size/mm	0.19 × 0.12 × 0.10	0.12 × 0.11 × 0.08	0.13 × 0.11 × 0.09
Reflections collected	24 448	8374	12 840
Independent reflections	8122	3109	7842
	$R_{int} = 0.0742$	$R_{int} = 0.0518$	$R_{int} = 0.0421$
Data/restraints/parameters	8122/0/451	3109/36/262	7842/32/448
Goodness-of-fit on F^2	1.047	1.117	1.005
Final R indices [$I > 2\sigma(I)$]^a	$R1 = 0.0448$	$R1 = 0.0525$	$R1 = 0.0468$
	w$R2 = 0.0778$	w$R2 = 0.1315$	w$R2 = 0.1019$
R indices (all data)^b	$R1 = 0.0953$	$R1 = 0.0750$	$R1 = 0.0898$
Max./min. residual electron densities/e Å^{-3}	1.281/−1.175	2.075/−2.127	1.104/−0.768

^{a} $R = \sum||F_o| - |F_c||/\sum|F_o|$ for all $I > 2\sigma(I)$. ^{b} w$R = [\sum w(|F_o| - |F_c|)^2/\sum wF_o^2]^{\frac{1}{2}}$.

1.95 (m, 2H, –CH_2–), 1.87 (m, 2H, –CH_2–), 1.71 (m, 2H, –CH_2–), 1.67 (m, 2H, –CH_2–). ^{13}C NMR (75 MHz, CDCl$_3$): δ 180.2 (NCN–Ir), 137.5 (–CH=CH$_2$), 120.2 (–NCHCHN–), 115.8 (–CH=CH$_2$), 84.3 (COD), 51.6 (COD), 50.8 (2C, NCH$_2$), 33.8 (COD), 31.0 (COD), 30.2 (–CH$_2$–), 29.7 (–CH$_2$–). ESI-MS (cone 25 V): m/z (fragment) 505.3 [M − Cl$^+$].

Structure determination and refinement of complexes 2a, 2b · PF$_6$ and 3‡. General procedure: A single crystal was mounted on a glass fiber in a random orientation. Data collection was performed at room temperature on a Siemens Smart CCD diffractometer using graphite monochromated Mo-K$_\alpha$ radiation (λ = 0.71073 Å) with a nominal crystal-to-detector distance of 4.0 cm. A hemisphere of data was collected based on three ω-scan runs (starting ω = −28°) at values ϕ = 0, 90 and 180, with the detector at 2θ = 28° In each of these runs, frames (606, 435 and 230, respectively) were collected at 0.3° intervals with 40 s per frame. Space group assignments are based on systematic absences, E statistics and the successful refinement of the structures. Structures were solved by direct methods with the aid of successive difference Fourier maps and were refined using the SHELXTL 5.1 software package.[21] All non-hydrogen atoms were refined anisotropically. Hydrogen atoms were assigned to ideal positions and refined using a riding model. Therefore, no reliance should be placed on the reported ethylenic hydrogen atom coordinates. Details of the data collection, structure refinement and cell dimensions are given in Table 3. The diffraction frames were integrated using the SAINT package and corrected for absorption with SADABS.[22]

References

1 B. Marciniec, J. Gulinski, W. Urbaniac and Z. W. Kornetka, *Comprehensive Handbook on Hydrosilylation*, Pergamon, Oxford, 1992.
2 M. A. Brook, *Silicon in Organic, Organometallic and Polymer Chemistry*, John Wiley & Sons, New York, 2000.
3 *Organosilicon Chemistry VI: From Molecules to Materials*, ed. N. Auner and J. Weiss, Wiley-VCH, Weinheim, 2005.
4 (*a*) W. A. Herrmann, *Angew. Chem., Int. Ed.*, 2002, **41**, 1291–1309; (*b*) D. Bourissou, O. Guerret, F. P. Gabbai and G. Bertrand, *Chem. Rev.*, 2000, **100**, 39–91; (*c*) C. M. Crudden and D. P. Allen, *Coord. Chem. Rev.*, 2004, **248**, 2247–2273; (*d*) E. Peris and R. H. Crabtree, *C. R. Chim.*, 2003, **6**, 33–37.
5 (*a*) R. Dorta, E. D. Stevens, N. M. Scott, C. Costabile, L. Cavallo, C. D. Hoff and S. P. Nolan, *J. Am. Chem. Soc.*, 2005, **127**, 2485–2495; (*b*) J. K. Huang, H. J. Schanz, E. D. Stevens and S. P. Nolan, *Organometallics*, 1999, **18**, 5375–5380; (*c*) G. D. Frey, C. F. Rentzsch, D. von Preysing, T. Scherg, M. Muhlhofer, E. Herdtweck and W. A. Herrmann, *J. Organomet. Chem.*, 2006, **691**, 5725–5738.
6 (*a*) J. A. Mata, M. Poyatos and E. Peris, *Coord. Chem. Rev.*, 2007, **251**, 841–859; (*b*) E. Peris and R. H. Crabtree, *Coord. Chem. Rev.*, 2004, **248**, 2239–2246.
7 J. A. Mata, A. R. Chianese, J. R. Miecznikowski, M. Poyatos, E. Peris, J. W. Faller and R. H. Crabtree, *Organometallics*, 2004, **23**, 1253–1263.
8 (*a*) M. Viciano, E. Mas-Marza, M. Sanau and E. Peris, *Organometallics*, 2006, **25**, 3063–3069; (*b*) E. Mas-Marza, M. Poyatos, M. Sanau and E. Peris, *Inorg. Chem.*, 2004, **43**, 2213–2219; (*c*) E. Mas-Marza, M. Sanau and E. Peris, *Inorg. Chem.*, 2005, **44**, 9961–9967.

9 C. Vicent, M. Viciano, E. Mas-Marza, M. Sanau and E. Peris, *Organometallics*, 2006, **25**, 3713–3720.
10 F. E. Hahn, C. Holtgrewe, T. Pape, M. Martin, E. Sola and L. A. Oro, *Organometallics*, 2005, **24**, 2203–2209.
11 F. E. Hahn, B. Heidrich, T. Pape, A. Hepp, M. Martin, E. Sola and L. A. Oro, *Inorg. Chim. Acta*, 2006, **359**, 4840–4846.
12 M. J. Doyle and M. F. Lappert, *J. Chem. Soc., Chem. Commun.*, 1974, 679–680.
13 A. R. Chianese, X. W. Li, M. C. Janzen, J. W. Faller and R. H. Crabtree, *Organometallics*, 2003, **22**, 1663–1667.
14 (*a*) D. Enders and H. Gielen, *J. Organomet. Chem.*, 2001, **617**, 70–80; (*b*) D. Enders, H. Gielen, J. Runsink, K. Breuer, S. Brode and K. Boehn, *Eur. J. Inorg. Chem.*, 1998, 913–919.
15 (*a*) F. A. Jalon, B. R. Manzano, F. Gomez-de la Torre, A. M. Lopez-Agenjo, A. M. Rodriguez, W. Weissensteiner, T. Sturm, J. Mahia and M. Maestro, *J. Chem. Soc., Dalton Trans.*, 2001, 2417–2424; (*b*) M. V. Galakhov, G. Heinz and P. Royo, *Chem. Commun.*, 1998, 17–18; (*c*) C. P. Casey, M. A. Fagan and S. L. Hallenbeck, *Organometallics*, 1998, **17**, 287–289.
16 R. Corberan, M. Sanau and E. Peris, *Organometallics*, 2007, **26**, 3492–3498.
17 (*a*) I. E. Marko, S. Sterin, O. Buisine, R. Mignani, P. Branlard, B. Tinant and J. P. Declercq, *Science*, 2002, **298**, 204–206; (*b*) G. De Bo, G. Berthon-Gelloz, B. Tinant and I. E. Marko, *Organometallics*, 2006, **25**, 1881–1890; (*c*) V. Cesar, S. Bellemin-Laponnaz, H. Wadepohl and L. H. Gade, *Chem.–Eur. J.*, 2005, **11**, 2862–2873.
18 V. Lillo, J. Mata, J. Ramirez, E. Peris and E. Fernandez, *Organometallics*, 2006, **25**, 5829–5831.
19 (*a*) M. Poyatos, E. Mas-Marza, J. A. Mata, M. Sanau and E. Peris, *Eur. J. Inorg. Chem.*, 2003, 1215–1221; (*b*) M. Poyatos, P. Uriz, J. A. Mata, C. Claver, E. Fernandez and E. Peris, *Organometallics*, 2003, **22**, 440–444; (*c*) M. Poyatos, A. Maisse-Francois, S. Belle-min-Laponnaz and L. H. Gade, *Organometallics*, 2006, **25**, 2634–2641.
20 A. J. Arduengo, *US Pat.*, 6 177575, 2001.
21 G. M. Sheldrick, *SHELXTL v 5.1*, Bruker AXS, Inc., Madison, WI, 1997.
22 (*a*) *SAINT v 5.0*, Bruker Analytical X-Ray Systems, Madison, WI, 1998; (*b*) G. M. Sheldrick, *SADABS: Empirical Absorption Program*, University of Göttingen, Göttingen, Germany, 1996.